NEPHROLOGY

Openventio PUBLISHERS

ISSN 2380-0445 Open Journal http://dx.doi.org/10.17140/NPOJ-3-116

Research

*Corresponding author
VK Subramanian, PhD
Assistant Professor
Department of Chemistry
Annamalai University
Annamalai Nagar, TN 608002, India
Tel. 0091 9486282324
E-mail: drvksau@gmail.com

Volume 3 : Issue 1
Article Ref. #: 1000NPOJ3116

Article History
Received: May 9th, 2017
Accepted: July 6th, 2017
Published: July 6th, 2017

Citation
Nirmaladevi M, Sanjiv Raj K, Subramanian VK. Effect of diethylenetriaminepentaacetic acid (DTPA) on crystal growth and morphology of calcium oxalate. *Nephrol Open J.* 2017; 3(1): 1-8. doi: 10.17140/NPOJ-3-116

Copyright
©2017 Subramanian VK. This is an open access article distributed under the Creative Commons Attribution 4.0 International License (CC BY 4.0), which permits unrestricted use, distribution, and reproduction in any medium, provided the original work is properly cited.

Effect of Diethylenetriaminepentaacetic Acid (DTPA) on Crystal Growth and Morphology of Calcium Oxalate

Muthulingam Nirmaladevi, MSc; Kumar Sanjiv Raj, MSc, MPhil; Vadakkeputhanmadom Krishnayer Subramanian, PhD*

Department of Chemistry, Annamalai University, Annamalai Nagar, TN 608002, India

ABSTRACT

Introduction: One of the most common and painful diseases observed in the tropical regions is kidney stone formation. This can be due to various factors such as the amount of water consumption, climatic conditions, lifestyle and diet. Although, kidney stones are composed of calcium phosphate were only found to be 10%, it has been observed that the deposition of such stones have been increasing steadily for the past 30 years in females.
Aim: To study the effects of diethylenetriaminepentaacetic acid (DTPA) on crystal growth and morphology of calcium oxalate.
Materials and Methods: Calcium oxalate was synthesized from calcium chloride solution using oxalic acid in the presence of DTPA at different concentrations. The experiments were carried out at 60 °C. The samples were characterized using powder X-ray diffraction analysis (XRD), Fourier transform infrared spectroscopy (FTIR) and scanning electron microscope (SEM) techniques.
Results: The study revealed that in the absence of DTPA, samples exhibited flower like morphology by agglomeration of rod like basic blocks and the tendency for agglomeration decreases with increase in DTPA concentration.
Conclusion: Interpretation of XRD pattern confirmed that whewellite with a monoclinic structure is the most favoured structure in the absence of DTPA where as calcium oxalate hydrate having orthorhombic structure is most favoured structure in the presence of DTPA.

KEY WORDS: Calcium oxalate; Kidney stone; Chelation therapy; Crystal growth; Fourier transform infrared spectroscopy; Scanning electron microscope; X-ray diffraction; DTPA.

ABBREVIATIONS: DTPA: Diethylenetriaminepentaacetic Aacid; XRD: X-ray diffraction analysis; FTIR: Fourier Transform Infrared Spectroscopy; SEM: Scanning Electron Microscop; COM: Calcium Oxalate Monohydrate; COD: Calcium Oxalate Dihydrate.

INTRODUCTION

Deposition of stones in kidney is one of the most common and painful diseases particularly in tropical regions. Various factors such as consumption of water, its quality, climate, lifestyle and diet can affect the formation and type of kidney stone. Majority of the kidney stones are composed of calcium, which may be in the form of calcium oxalate (70-80%) or calcium phosphate (10%) or mixture of both (40-50%).[1-4] However, calcium phosphate stone composition has been increasing steadily for the past 30 years with female predominance.[5] Apart from inorganic composition, kidney stones may also contain organic matrix accounting for 2-5% of the total stone weight.[6,7]

Even though calcium oxalate exists in both monohydrate (COM) and dihydrate (COD) crystal phases, several studies have reported that the precipitate in the urinary tract consists of COM, having a greater stone forming tendency than COD[4] and that all papillary stones are

Openventio PUBLISHERS

ISSN 2380-0445 http://dx.doi.org/10.17140/NPOJ-3-116

COM stones.[8,9] The stone forming process is highly complex involving nucleation, crystal growth, and aggregation of crystals in an environment containing supersaturated crystal-forming ions (e.g. Ca^{2+}, $C_2O_4^{2-}$, PO_4^{3-}, Mg^{2+}, SO_4^{2-}) in the presence of promoters and inhibitors.[10] The acid-rich urinary proteins suppress the crystallization of calcium oxalate even under supersaturated conditions,[11] thus preventing the formation of stones. Chelation therapy is one of the recent techniques for the treatment of many diseases including kidney stones.[12] Preferential crystallization of different forms of calcium oxalate has been reported by many researchers by using certain synthetic and natural molecules, such as polypeptides,[13,14] sodium diisooctylsulfosuccinate,[15] poly (ethyleneglycol)-block-poly (methacrylic acid),[16] renal epithelial cells,[17,18] poly (sodium 4-styrene-sulfonate),[19] biopolymeric additives,[20] and protein isolated from bean seed coats.[21]

Reports by Shinichi et al suggest that the conventional homogeneous precipitation results into monohydrate and granular calcium oxalate. However, hydrolysis of oxamic acid catalyzed by enzyme (hydrolase) generates trihydrate and fibrous calcium oxalate.[22] Recent studies carried out on synthesis of $CaCO_3$ revealed that the crystalline structure of calcium carbonate particles mainly depend on the precipitation condition, such as pH, temperature and presence of sequestrants, etc.[23-30]

The above survey revealed that effect of the presence of calcium ions in water on the formation of calcium oxalate while using oxalic acid has not been reported so far. In this paper we describe the effects of diethylenetriaminepentaacetic acid (DTPA), a chelating agent, on the morphology and structure of calcium oxalate precipitated from calcium chloride solution using oxalic acid. The results indicate that morphology and structure of the resulted calcium oxalate vary with the conditions. The architecture of the samples shows that DTPA has significant influence on the morphology and crystalline structure of calcium oxalate.

EXPERIMENTAL DETAILS

Reagents and Materials

Analytical grade $CaCl_2$, DPTA and $Na_2C_2O_4$ were obtained from Sigma-Aldrich chemical company, Bengaluru, KA, India. The reagents were used as such. Double distilled water was used for the preparation of aqueous solutions. Analytical grade 1:1 ammonia and acetic acid were used to adjust the pH whenever necessary.

Methodology

Experiments were carried out in a similar fashion as explained by Vijaya et al.[31] Precipitation was carried out from a 0.1 M $CaCl_2$ solution using 0.1 M oxalic acid at 60 °C. In a typical synthesis, 50 ml of $CaCl_2$ solution was taken in a round bottom flask and 50 ml DTPA was added. The pH was adjusted to 7. The solution was heated to 60 °C and 50 ml oxalic acid was added from a burette. The mixture was kept at 60 °C for a period of 12 h and the precipitate obtained was filtered using Watman No. 40 filter paper. It was dried at 40 °C and then kept in a desiccator.

The pH measurements were made using Elico pH meter, model LI-120. FT-IR spectra were taken in the range 500-4000 cm^{-1} using Avatar-330 FTIR spectroscopy after KBr pelletization. Microscopic morphological structure measurements were performed with Jeol JSM 5610 LV scanning electron microscope (SEM). The samples were coated with Au prior to examination. The powder X-ray diffraction (XRD) patterns were recorded on an INEL Equinox 1000 Advanced XRD diffractometer with Cu Ka radiation at k=1.5406 Å.

RESULTS AND DISCUSSIONS

Interpretation of Powder XRD Data

Figures 1a, 1b, 1c, 1d and 1e represents the XRD pattern of the samples. Figure 1a depicts the XRD pattern of the blank samples; i.e. prepared in the absence of DTPA. The data confirms the presence of calcium oxalate in the form of whewellite (calcium oxalate hydrate) vide JCPDS card 78-6695. The cell parameters a, b and c are 9.9780, 7.295 and 6.292 respectively which confirmed that the samples exhibit monoclinic structure.

The XRD pattern of sample prepared in the presence of 10, 20, 30 and 40 ml DTPA are presented in Figure 1b, 1c, 1d and 1e respectively. The powder XRD pattern of samples showed the existence of calcium oxalate in the form of monoclinic. The samples with 10 ml and 20 ml DTPA had same cell parameters; a, b and c as 9.794, 14.74 and 6.306 respectively and were matching with joint committee on powder diffraction standards (JCPDS) card 20-0231. The sample synthesized in presence of 30 ml DTPA had cell parameters; a, b and c as 9.796, 7.294 and 6.291 respectively and were in good agreement with JCPDS card 20-0231. The cell parameters of the sample synthesized in presence of 40 ml DTPA were different from the above and were 9.976, 7.294 and 6.291 for a, b and c respectively and were in good agreement with JCPDS card 20-0231.

Although, the positions of the peaks (°2θ) in the XRD pattern of all the samples correspond to whewellite and match very well with each other, the ratio of their intensities of the samples prepared in the presence of DTPA varied much from the blank sample. In the absence of DTPA, the two peaks around °2θ~15 and 24.5 showed similar intensities. With 10 ml and 20 ml DTPA, the peak at °2θ~24.5 was more intense than the peak around °2θ~15. With higher concentrations of DTPA (30 and 40 ml), the peak at °2θ~1.5 was more intense than the peak around °2θ~24.5. This indicates that the crystalline nature of the samples varied with the environment and the degree of crystallinity was affected much by the presence of DTPA.

Interpretation of FTIR

Aslin et al[32] have reported the physicochemical analysis of urinary stones from Dharmapuri district in India. They have char-

NEPHROLOGY
Open Journal

Openventio PUBLISHERS

ISSN 2380-0445

http://dx.doi.org/10.17140/NPOJ-3-116

Figure 1a: XRD Pattern of Calcium Oxalate Sample Synthesized in the Absence of DTPA.

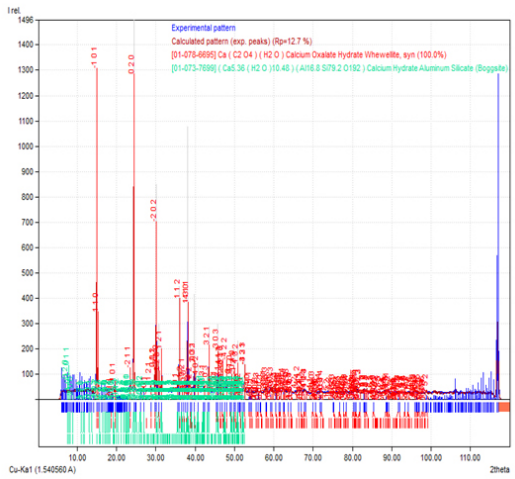

Figure 1b: XRD Pattern of Calcium Oxalate Sample Synthesized in the Presence of 10 ml DTPA.

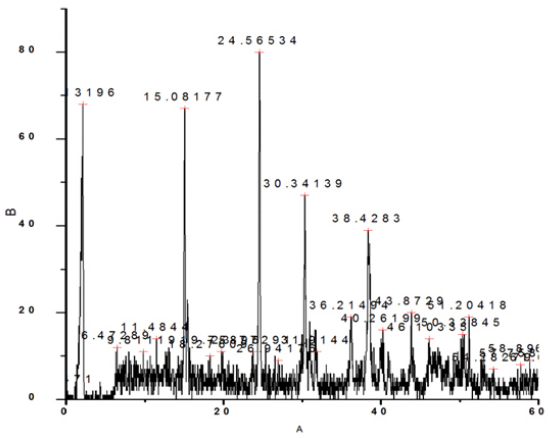

Figure 1c: XRD Pattern of Calcium Oxalate Sample Synthesized in the Presence of 20 ml DTPA.

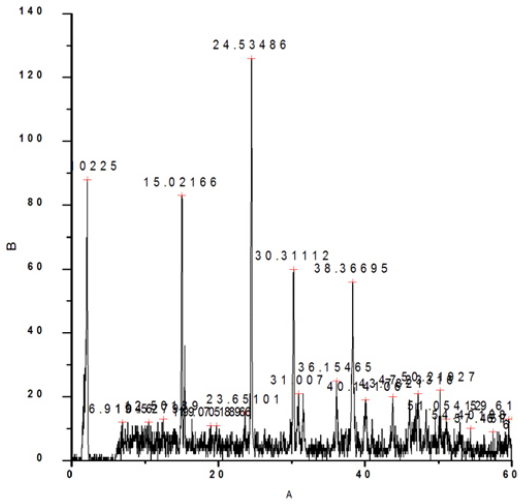

Figure 1d: XRD Pattern of Calcium Oxalate Sample Synthesized in the Presence of 30 ml DTPA.

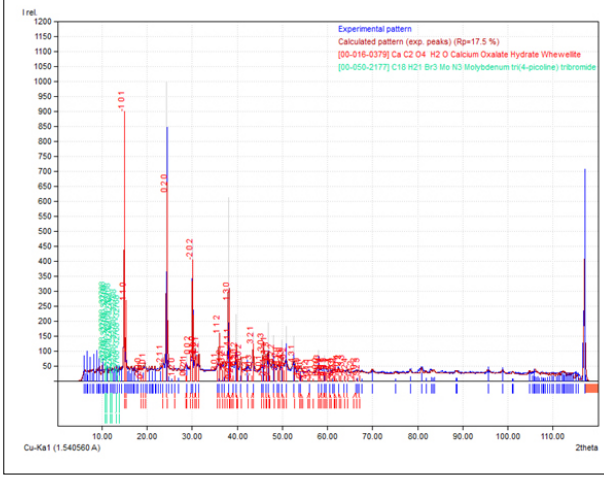

Figure 1e: XRD Pattern of Calcium Oxalate Sample Synthesized in the Presence of 40 ml DTPA.

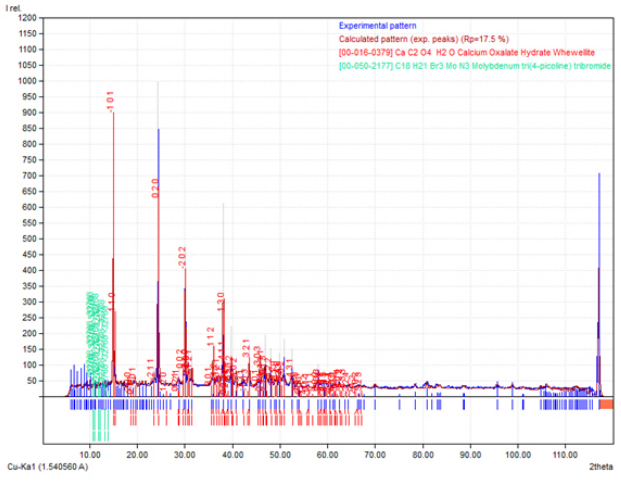

NEPHROLOGY
Open Journal
Openventio PUBLISHERS
ISSN 2380-0445
http://dx.doi.org/10.17140/NPOJ-3-116

acterized functional groups and phases of the stones using X-ray diffraction (XRD), Fourier transform Raman spectroscopy and Fourier transform infrared spectroscopy (FT-IR). Their study revealed that the majority of the stones were found to be calcium oxalate monohydrate (COM) and mixed stones had a minor existence of struvite and uric acid.

The FTIR spectrum of the blank sample as well as with 10, 20, 30 and 40 ml DTPA are shown in Figure 2a, 2b, 2c, 2d and 2e respectively. The characteristic bands assigned for sample without DTPA (Figure 2a) are 511 cm^{-1} to O-C-O in-plane bending , 660 cm^{-1} to weak band bending and wagging modes, 774 cm^{-1} (O-C=O), 954 cm^{-1} sym C-O stretch, 1319 sym C=O stretch, 1603 C-O stretch, 1784cm^{-1}, 3023 cm^{-1} symmetric and asymmetric O-H stretching.

The sample prepared in the presence of 10 ml DTPA exhibited frequencies at 511 cm^{-1} corresponding to O-C-O in-plane bending , 660 cm^{-1} weak band bending and wagging modes, 774 cm^{-1} (O-C=O), 888 cm^{-1} C-C stretch (rocking mode of water), 954 cm^{-1} sym C-O stretch, 1307 sym C=O stretch, 1603 C-O stretch, 1784 cm^{-1}, 3047 cm^{-1}, 3239 cm^{-1}, 3331 cm^{-1}, 3421 cm^{-1}, 3500 cm^{-1} symmetric and asymmetric O-H stretching.

The bands observed for 20 ml DTPA (Figure 2c) are 511 cm^{-1} O-C-O in plane bending, 660 cm^{-1} weak band bending and wagging modes, 784 cm^{-1} (O-C=O), 888 cm^{-1} C-C stretch (rocking mode of water), 954 cm^{-1} sym C-O stretch, 1307 sym C=O stretch, 3056 cm^{-1}, 3250 cm^{-1}, 3331 cm^{-1}, 3433 cm^{-1}, 3490 cm^{-1} symmetric and asymmetric O-H stretching.

Figure 2d shows the FTIR of the sample synthesized in presence of 30 ml DTPA. Characteristic bands were observed at 511 cm^{-1} O-C-O in-plane bending , 660 cm^{-1} weak band bending and wagging modes, 772 cm^{-1}(O-C=O), 886 cm^{-1} C-C stretch (rocking mode of water), 954 cm^{-1} sym C-O stretch , 1307 sym C=O stretch, 1613 C-O stretch, 3045 cm^{-1}, 3250 cm^{-1}, 3329 cm^{-1}, 3488 cm^{-1} symmetric and asymmetric O-H stretching.

The calcium oxalate synthesized in presence of 50 ml DTPA exhibited FTIR bands at 511 cm^{-1} O-C-O in plane-bending , 660 cm^{-1} weak band bending and wagging modes, 784 cm^{-1}

Figure 2a: FTIR of Calcium Oxalate Sample Synthesized in the Absence of DTPA.

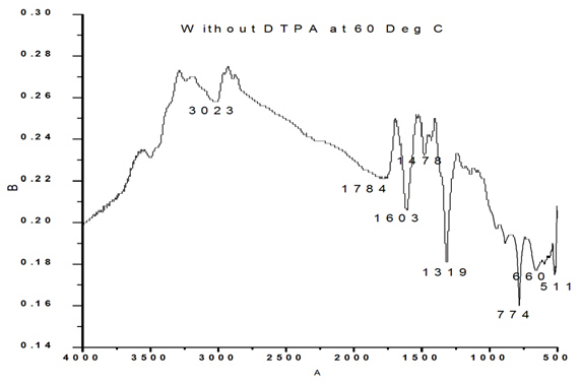

Figure 2b: FTIR of Calcium Oxalate Sample Synthesized in the Presence of 10 ml DTPA.

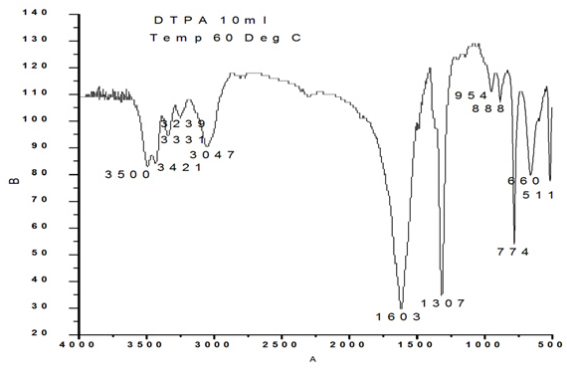

Figure 2c: FTIR of Calcium Oxalate Sample Synthesized in the Presence of 20 ml DTPA.

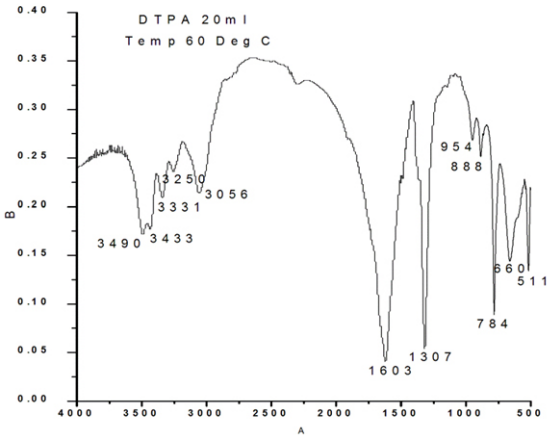

Figure 2d: FTIR of Calcium Oxalate Sample Synthesized in the Presence of 30 ml DTPA.

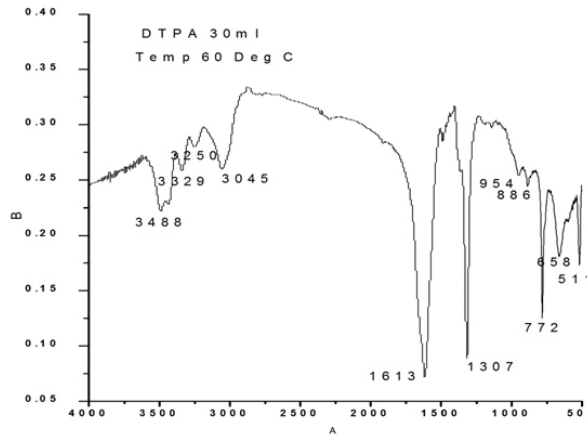

Openventio PUBLISHERS

ISSN 2380-0445 http://dx.doi.org/10.17140/NPOJ-3-116

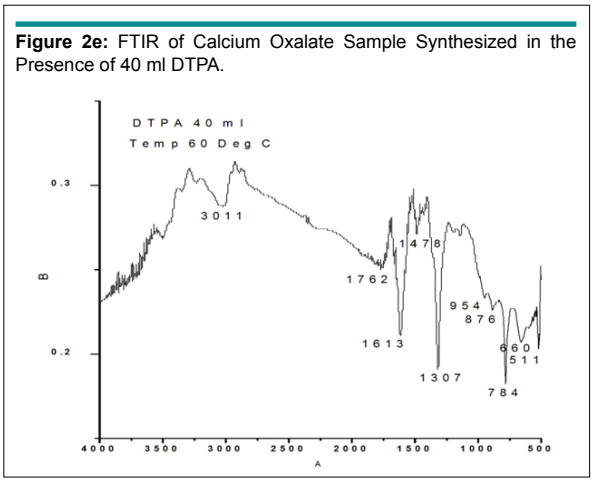

Figure 2e: FTIR of Calcium Oxalate Sample Synthesized in the Presence of 40 ml DTPA.

[1](O-C=O), 876 cm^{-1} C-C stretch (rocking mode of water), 954 cm^{-1} sym C-O stretch, 1307 sym C=O stretch, 1613 C-O stretch, 3011 cm^{-1} symmetric and asymmetric O-H stretching.

It is obvious from the above data that in the absence of DTPA, frequencies/bands corresponding to C-C stretch (rocking mode of water) and sym C-O stretch at around 886 cm^{-1} and 954 cm^{-1} are absent. Similarly, the band around 1478 cm^{-1} is absent in all samples prepared in the presence of DTPA except with 40 ml. This band can be attributed to in-plane bending of CO (v). Again the bands around 511 cm^{-1} and 660 cm^{-1} are distinct and clear in the case of samples with 10, 20 and 30 ml DTPA. The intensities of these peaks decreased in blank as well as in the 40 ml DTPA sample. Analysis of urinary stone constituents using powder X-ray diffraction and FT-IR has been reported by Pragnya Bhatt and Parimal Paul.[33] They have reported the presence of the apatite phase with an uncertainty on whether it has formed independently or the calcium oxalate monohydrate phase has been transformed into these phases with time. Similarly, in our study, in the case of 40 ml, there could be a possibility of the formation of an apatite phase with the transformation of calcium oxalate monohydrate phase with time.

Interpretation of SEM Images

Figure 3a and 3b show the SEM images of sample prepared in the absence of DTPA. Flower like morphology formed by the interlinking of petals ranging from about 5-10 µm length and width of about 1 µm were observed under these conditions. The images also showed indications of smaller units exhibiting agglomeration at the centre of this structure or at the junction of cross linking (Figure 3b). The morphology of sample prepared with 10 ml DTPA are depicted in Figure 3c and 3d. They showed similarity with that of samples without DTPA. However, the tendency of agglomeration or degree of cross linking was comparatively less. Unlike the blank sample (without DTPA), it could be noticed from the SEM image (Figure 3b) that all the crystallites did not show flower like morphology. Some of the crystallites had only 4/6 petal like blocks attached to form the flower. In the sample without DTPA, the numbers of blocks to form agglomeration were too many. Some loose blocks were also seen in this image.

The sample prepared with 20 ml DTPA exhibited marked difference in the morphology. The flower like morphology was quite fewer in number. Majority of the crystallites exhibited block like structures (Figure 3e).

It could be observed from the magnified image (Figure 3f) that these blocks resulted from rod like structures. On increasing the DTPA concentration to 30 ml, the flower like morphology reappeared again (Figure 3g) along with the rod like

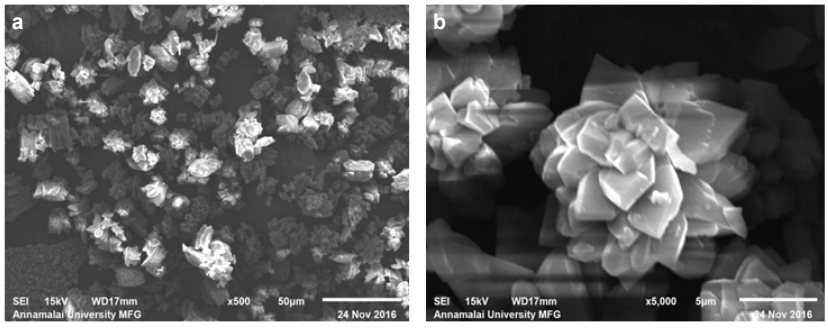

Figure 3(a,b): SEM Omages of Calcium Oxalate Sample Synthesized in the Absence of DTPA.

Openventio PUBLISHERS

ISSN 2380-0445 http://dx.doi.org/10.17140/NPOJ-3-116

Figure 3(c,d): SEM Images of Calcium Oxalate Sample Synthesized in the Presence of 10 ml DTPA.

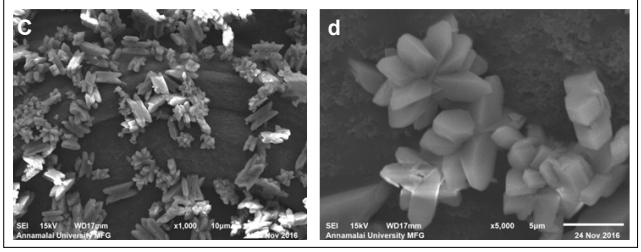

Figure 3(e,f): SEM Images of Calcium Oxalate Sample Synthesized in the Presence of 20 ml DTPA.

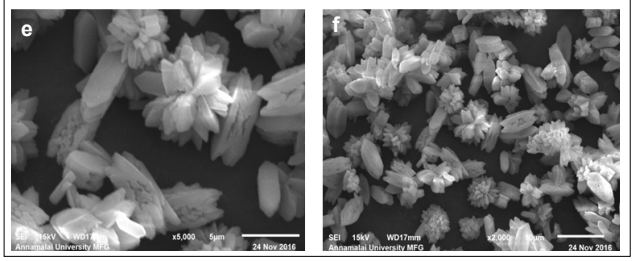

Figure 3(g,h): SEM Images of Calcium Oxalate Sample Synthesized in the Presence of 30 ml DTPA.

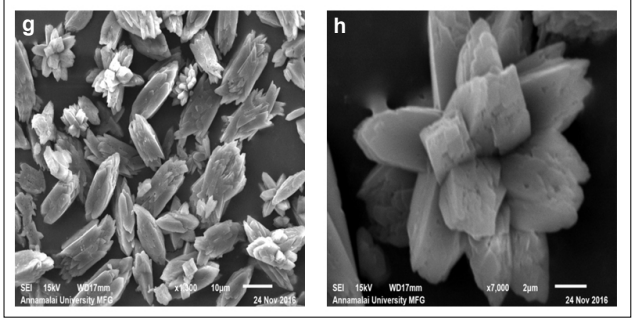

Figure 3(i,j): SEM Images of Calcium Oxalate Sample Synthesized in the Presence of 40 ml DTPA.

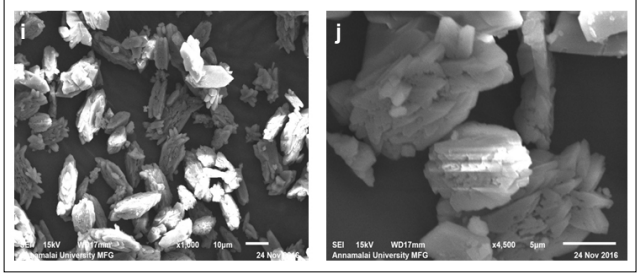

crystallites. However, with 30 ml DTPA, the flower like morphology was equal in numbers with the rod like crystallites. The rod like morphology showed tendency for sharp ends leading to an ellipsoidal shape. The trend continued with increase in DTPA concentration. With 40 ml DTPA, the dual morphology continued to exist. The number of ellipsoidal particles increased and the flower like structures reduced in numbers.

Mechanism of Formation of Flower Like and Block Like Structures

On the basis of the above experimental results, the mechanism of formation of this flower structure of calcium oxalate can be explained as follows: The crystallization of calcium oxalate in the absence of DTPA forms these basic blocks with rod like structures. From the SEM images (Figure 3a, 3b) it could be observed that there are no free building blocks in the images. This shows that the agglomeration is uninhibited in the absence of DTPA. Usually, the crystal growth is governed by both kinetic and thermodynamic factors. The observed flower morphology reflects the relative rates of growth of the crystal to different directions in the absence of DTPA. It is expected that in the absence of DTPA, more sites are available for further agglomeration or joining (Figure 3b). However, the presence of DTPA, which forms a complex with calcium, inhibits this tendency and the sites for growth could not go beyond a certain number. This is clearly observable in Figure 3c, 3d and further images, where the number of petals are few when compared to that of the blank. The above mechanism of inhibition of agglomeration or joining is further inhibited with the rise in concentration of DTPA and is evident from the SEM images of calcium oxalate synthesized in the presence of 30 and 40 ml DTPA.

CONCLUSION

The above observations indicate that DTPA strongly influences the crystallization of calcium oxalate. The study revealed that the crystallization process of calcium oxalate is entirely different in presence of DTPA. Whewellite with monoclinic structure is the most favoured polymorph in the absence of DTPA, where as calcium oxalate hydrate with an orthorhombic structure is the most favoured structure in the presence of DTPA. With increase in DTPA concentrations, there is significant difference in the morphology and the dual morphology was predominant. Similarly, the unit structures showed an increased tendency of cross linking in the absence of DTPA. These results could be helpful to understand the effects of DTPA on crystal growth of calcium oxalate based kidney stone and form a basis for the further studies on chelation therapy using DTPA and other chelating agents.

CONFLICTS OF INTEREST

The authors declare that they have no conflicts of interest.

REFERENCES

1. Bihl G, Meyers A. Recurrent renal stone disease-advances in pathogenesis and clinical management. *Lancet*. 2001; 358(9282): 651-656. doi: 10.1016/S0140-6736(01)05782-8

2. Reynolds TM. Chemical pathology clinical investigation and management of nephrolithiasis. *J Clin Pathol*. 2005; 58(2): 134-140. doi: 10.1136/jcp.2004.019588

3. Bushinsky DA. Kidney stones. *Adv Intern Med*. 2001; 47:

ISSN 2380-0445 http://dx.doi.org/10.17140/NPOJ-3-116

219-238.

4. Lieske JC, Toback FG. Renal cell-urinary crystal interactions. *Curr Opin Nephrol Hypertens*. 2000; 9: 349-355.

5. Parks JH, Worcester EM, Coe FL, Evan AP, Lingeman JE. Clinical implications of abundant calcium phosphate in routinely analyzed kidney stones. *Kidney Int*. 2004; 66(2): 777-785. doi: 10.1111/j.1523-1755.2004.00803.x

6. King JS, Boyce WH. Immunological studies on serum and urinary proteins in urolith matrix in man. *Ann N Y Acad Sci*. 1963; 104: 5791.

7. Robertson WG, Peacock M, Nordin BEC. Activity products in stone-forming and non-stone-forming urine. *Clin Sci*. 1968: 34(3): 579-594.

8. Grases F, Costa-Bauzá A, Bonarriba CR, Pieras EC, Fernández RA, Rodríguez A. On the origin of calcium oxalate monohydrate papillary renalstones. *Urolithiasis*. 2015; 43: S33-S39. doi: 10.1007/s00240-014-0697-5

9. Evan AP, Worcester EM, Coe FL, Williams J Jr, Lingeman JE. Mechanisms of human kidney stone formation. *Urolithiasis*. 2015; 43(Suppl 1): 19-32. doi: 10.1007/s00240-014-0701-0

10. Khan SR, Kok DJ. Modulators of urinary stone formation. *Front Biosci*. 2004; 9: 1450-1482. doi: 10.2741/1347

11. Jung T, Woo-Sik K, Choia CK. Crystal structure and morphology control of calcium oxalate using biopolymeric additives in crystallization. *Journal of Crystal Growth*. 2005; 279(1-2): 154-162. doi: 10.1016/j.jcrysgro.2005.02.010

12. Poon NW, Gohel MD, Lau C, Hon EK, Leung PC, Ng CF. Melamine crystallization: Physicochemical properties, interactions with other lithogenic salts and response to therapeutic agents. *J Urol*. 2012; 187(4): 1483-1490. doi: 10.1016/j.juro.2011.11.078

13. Wesson JA, Worcester E. Formation of hydrated calcium oxalates in the presence of poly-L-aspartic acid. *Scanning Microsc*. 1996; 10(2): 415-423; 423-424.

14. Wesson JA, Worcester EM, Kleinman JG. Role of anionic proteins in kidney stone formation: Interaction between model anionic polypeptides and calcium oxalate crystals. *J Urol*. 2000; 163(4): 1343-1348. doi: 10.1016/S0022-5347(05)67775-0

15. Tunik L, Füredi-Milhofer H, Garti N. Adsorption of sodium diisooctyl sulfosuccinate onto calcium oxalate crystals. *Langmuir*. 1998; 14(12): 3351-3355. doi: 10.1021/la9708041

16. Zhang D, Qi L, Ma J, Cheng H. Morphological control of calcium oxalate dihydrate by a double-hydrophilic block copolymer. *Chem Mater*. 2002; 14(6): 2450-2457. doi: 10.1021/cm010768y

17. Lieske JC, Toback FG, Deganello S. Sialic acid-containing glycoproteins on renal cells determine nucleation of calcium oxalate dihydrate crystals. *Kidney Int*. 2001; 60(5): 1784-1791. doi: 10.1046/j.1523-1755.2001.00015.x

18. Lieske JC, Toback FG, Deganello S. Face-selective adhesion of calcium oxalate dihydrate crystals to renal epithelial cells. *Calcif Tissue Int*. 1996; 58(3): 195-200. doi: 10.1007/BF02526887

19. Yu J, Tang H, Cheng B. Influence of PSSS additive and temperature on morphology and phase structures of calcium oxalate. *J Colloid Interface Sci*. 2005; 288(2): 407-411. doi: 10.1016/j.jcis.2005.03.001

20. Jung T, Kim WS, Choi CK. Crystal structure and morphology control of calcium oxalate using biopolymeric additives in crystallization. *Journal of Crystal Growth*. 2005; 279(1-2): 154-162. doi: 10.1016/j.jcrysgro.2005.02.010

21. Jáuregui-Zúñigaa D, Reyes-Grajeda JP, Moreno A. Modifications on the morphology of synthetically-grown calcium oxalate crystals by crystal-associated proteins isolated from bean seed coats (*Phaseolus vulgaris*). *Plant Sci*. 2005; 168(5): 1163-1169. doi: 10.1016/j.plantsci.2004.12.013

22. Kato S, Unuma H, Takahashi M. Enzyme-catalyzed synthesis of hydrated calcium oxalate. *Advanced Powder Technology*. 2001; 12(4): 493-505. doi: 10.1163/15685520152756633

23. Gopi SP, Subramanian VK, Palanisamy K. Synergistic effect of EDTA and HEDP on the crystal growth, polymorphism, and morphology of $CaCO_3$. *Ind Eng Chem Res*. 2015; 54(14): 3618-3625. doi: 10.1021/ie5034039

24. Palanisamy K, Subramanian VK. $CaCO_3$ scale deposition on copper metal surface; Effect of morphology, size and area of contact under the influence of EDTA. *Powder Technology*. 2016; 294: 221-225. doi: 10.1016/j.powtec.2016.02.036

25. Palanisamy K, Sanjiv Raj K, Bhuvaneswari S, Subramanian VK. A novel phenomenon of effect of metal on calcium carbonate scale, morphology, polymorphism and its deposition. *Materials Research Innovations*. 2017; 21(5): 294-303. doi: 10.1080/14328917.2016.1214230

26. Palanisamy K, Sanjiv Raj K, Nirmala Devi M, Subramanian VK. Effect of EGTA and metal induced polymorphic selectivity of calcium carbonate scale on copper and aluminum. *Materials Discovery*. 2016; 4: 8-17. doi: 10.1016/j.md.2016.09.001

27. Naka K, Tanaka Y, Chujo Y, Ito Y. The effect of an anionic starburst dendrimer on the crystallization of $CaCO_3$ in aque-

ISSN 2380-0445 http://dx.doi.org/10.17140/NPOJ-3-116

ous solution *Chem Commun*. 1999; 1931-1932. doi: 10.1039/A905618A

28. Naka K, Keum DK, Tanaka Y, Chujo Y. Control of crystal polymorphs by a 'latent inductor': Crystallization of calcium carbonate in conjunction with in situ radical polymerization of sodium acrylate in aqueous solution. *Chem Commun*. 2000; 1537-1538. doi: 10.1039/B004649N

29. Kai A, Miki T. Hybrid crystals of calcium carbonate and amino acids. *J Appl Phys*. 2000; 39: 1071.

30. Manoli F, Dalas E. Calcium carbonate overgrowth on elastin substrate. *J Crystal Growth*. 1999; 204(3): 369-375. doi: 10.1016/S0022-0248(99)00175-X

31. Vijaya P, Gopi S, Wani AH, Rajasekharan MV, Subramanian VK. Effect of ethylenediaminetetraacetic acid (di sodium salt) and aquasoft 330 on crystal growth and morphology of calcium oxalate. *Advanced Powder Technology*. 2012; 23(6): 771-778. doi: 10.1016/j.apt.2011.10.006

32. Aslin Shamema A, Thanigai Arul K, Senthil Kumar R, Narayana Kalkura S. Physicochemical analysis of urinary stones from Dharmapuri district. *Spectrochim Acta A Mol Biomol Spectrosc*. 2015; 134: 442-448. doi: 10.1016/j.saa.2014.05.088

33. Bhatt PA, Paul P. Analysis of urinary stone constituents using powder X-ray diffraction and FT-IR. 2008; 120(2): 267-273.